Dyes and Pigments 82 (2009) 409–415

Contents lists available at ScienceDirect

Dyes and Pigments

journal homepage: www.elsevier.com/locate/dyepig

Monomethine cyanine dyes with an indole nucleus: Microwave-assisted solvent-free synthesis, spectral properties and theoretical studies

Yi-Le Fu [a], Wei Huang [a], Chun-Lan Li [a], Lan-Ying Wang [a,*], Yong-Sheng Wei [b], Yi Huang [b], Xiang-Han Zhang [a], Zhen-Yi Wen [c], Zu-Xun Zhang [a]

[a] Key Laboratory of Synthetic and Natural Functional Molecule Chemistry (Ministry of Education), College of Chemistry and Materials Science, Northwest University, Xian 710069, PR China
[b] Department of Chemistry, Xianyang Normal University, Xianyang, Shaanxi 712000, PR China
[c] Institute of Modern Physics, Northwest University, Xian 710069, PR China

ARTICLE INFO

Article history:
Received 11 August 2008
Received in revised form
4 March 2009
Accepted 5 March 2009
Available online 12 March 2009

Keywords:
Monomethine indocyanine dye
Microwave irradiation
UV–Vis spectra
IR spectra
TD-DFT/PCM

ABSTRACT

Four asymmetric monomethine indocyanine dyes were rapidly synthesized by the condensation of indole quaternary salts with 2-methylthio quinoline quaternary salt in the presence of triethylamine under solvent-free, microwave irradiation. The effects of microwave power and irradiation time on yield were examined. The products were identified using elemental analysis, IR, MS, UV–Vis spectra, ^{1}H and ^{13}C NMR. The absorption of the dyes was investigated both experimentally and theoretically. Calculations performed using a combination of the time-dependent density functional theory (TD-DFT) and the polarizable continuum model (PCM) reproduced the $\pi \rightarrow \pi^{*}$ type absorption bands of the dyes. Multiple linear regression, applied to the theoretical absorption maxima in different solvents, fitted well with experimental data. Resonance frequency calculations were undertaken to study the IR spectra of the dyes and the calculated results were in good accordance with experimental values.

1. Introduction

From a functional dye viewpoint, monomethine cyanine dyes have received much attention and have enjoyed practical application. Such dyes, which are characterized by large molar extinction coefficient, high fluorescence efficiency, large tunable range of maximum absorption wavelength, ease of synthesis and relatively high stability, have been widely used as spectral sensitisers [1], CD recording materials [2–4], biomedical applications [5–7], photodynamic therapy [8,9] and other application [10] in recent years.

In this paper, four asymmetric monomethine indocyanine dyes, three of which were unknown with the best of our knowledge, were rapidly synthesized under microwave irradiation without solvent (Fig. 1). The relationships among the reaction time, irradiation power and yield were inspected. The structure of products was confirmed with elemental analysis, IR, MS, UV–Vis spectra, ^{1}H and ^{13}C NMR. The approach provided an attractive and environment-friendly pathway to several synthetically useful monomethine cyanine dyes with indole nucleus.

Taking into account that the solvent can significantly influence the chemical and physical properties of the solute, the investigation of solvent–solute interactions is very important [11]. UV–Vis absorption spectral properties of four dyes (**5a**–**5d**) were studied by means of both experiment and TD-DFT [12–16] in this paper. The resonance frequency calculation of dye **5a** was carried out to do the preliminary study of its IR spectra. The calculated results were in good accordance with the experimental values. The goal of the research presented herein is to investigate the synthesis, structure and spectral properties of monomethine cyanine dyes with indole nucleus which has potential application in a number of fields.

2. Experimental

2.1. General

Melting points were taken on a XT-4 micro melting apparatus and uncorrected. IR (KBr pellets) spectra were recorded on a Brucker Equinox-55 spectrometer. ^{1}H and ^{13}C NMR spectra were recorded at 400 MHz on a Varian Inova-400 spectrometer and chemical shifts were reported relative to internal Me_4Si. Elemental analyses were performed with Vario EL-III instrument. The absorption spectra were recorded on a Shimadzu UV-1700 UV–Vis

* Corresponding author. Tel.: +86 29 88302604; fax: +86 29 88303798.
E-mail address: wanglany@nwu.edu.cn (L.-Y. Wang).

0143-7208/$ – see front matter © 2009 Elsevier Ltd. All rights reserved.
doi:10.1016/j.dyepig.2009.03.005

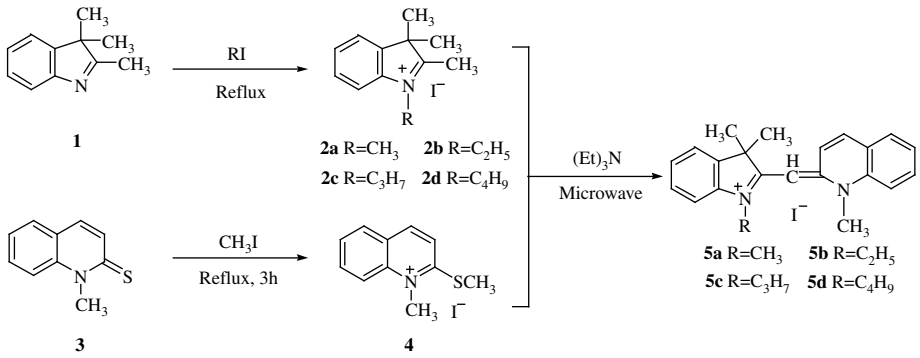

Fig. 1. Synthesis of monomethine indocyanine dyes.

spectrometer. MS spectra were recorded on a HP5973 MS spectrometer (American). All chemicals were of analytical grade.

2.2. Preparation of the quaternary salts **2a–2d** and **4**

The intermediates **2a–2d** were synthesized according to a revised literature procedure [17]. A mixture of 0.02 mol 2,3,3-trimethylindole, 0.03 mol methyl iodide and proper ethanol was reflux for 2 h. After the solvent was removed, the crude product was washed with ether and purified by recrystallization from ethanol.

The quinoline quaternary salt **4** was prepared by the modified literature method [18]. 0.028 mol 1-methyl-2-quinolinethione, 0.029 mol methyl iodide as well as proper amount of ethanol were mixed and heated for 3 h at 41 °C. After the solvent was removed, the product was purified by recrystallization from a mixed solvent of ethanol and acetone.

2.3. Preparation of dyes **5a–5d**

The condensation of indole quaternary salts and 2-methylthio quinoline quaternary salt was carried out in a Galanz microwave oven. 0.03 mol indole quaternary salt, 0.03 mol 2-methylthio quinoline quaternary salt and a few drops of triethylamine were mixed at ambient temperature in a glass conical flask. The mixture was subjected to microwave irradiation for a proper time and power. After cooling, the reaction mixture was recrystallized from ethanol to afford pure dyes **5a–5d**. The details of reaction conditions and yields are provided in Table 1 and the optimizing process for experimental condition of dye **5a** is listed in Table 2.

2.4. Structural confirmations

2.4.1. 1,1′3′,3′-Tetramethyl-indo-2-quinocyanine iodide (**5a**)

Salmon pink powder, m.p.: 253–254 °C (Ref. [19]: 256–257 °C). ^{1}H NMR (DMSO-d_6, 400 MHz) δ(ppm): 2.07 (s, 6H, C(CH_3)$_2$), 4.25 (s, 3H, NCH_3), 4.41 (s, 3H, N^+CH_3), 6.48 (s, 1H, –CH═), 7.51–7.53 (m, 1H, ArH), 7.59 (d, J = 8.0 Hz, 1H, ArH) 7.76–7.78 (m, 1H, ArH), 7.83 (d, J = 8.0 Hz, 1H, ArH), 7.92–7.94 (m, 2H, ArH), 7.97 (d, J = 8.0 Hz, 1H, ArH), 8.07 (d, J = 8.8 Hz, 1H, ArH), 8.11 (d, J = 8.0 Hz, 1H, ArH), 8.39 (d, J = 8.8 Hz, 1H, ArH). ^{13}C NMR ($CDCl_3$, 400 MHz) δ(ppm): 184.1, 151.7, 145.2, 144.3, 143.1, 136.4, 133.1, 129.1, 129.0, 128.7, 128.5, 128.4, 127.5, 126.0, 123.6, 121.8, 99.7, 56.2, 46.2, 31.7, 30.5, 30.2. IR (KBr) υ: 3010 (w, $\upsilon_{=CH}$), 2973, 2901 (m, υ_{C-H}), 1593, 1566, 1467, 1428 (s, $\upsilon_{C=C}$, $\upsilon_{C=N}$), 968 (m, $\delta_{=CH}$), 846, 805 (s, $\delta_{=CH}$) cm^{-1}. MS (70 eV) m/z (%): 300 (M–I–CH_3, 100), 172 (23), 157 (12), 143 (25), 142 (14), 127 (6), 115 (8), 77 (2), 51 (2). Anal. Calcd. for $C_{22}H_{23}N_2I$ = 442.34: C, 59.74; H, 5.24; N, 6.33; Found: C, 59.60; H, 5.19; N, 6.18. UV–Vis (MeOH) λ_{max}: 471 nm. ε: 4.60×10^4 L mol^{-1} cm^{-1}.

2.4.2. 1′-Ethyl-1,3′,3′-trimethyl-indo-2-quinocyanine iodide (**5b**)

Salmon pink powder, m.p.:235–236 °C. ^{1}H NMR (DMSO-d_6, 400 MHz) δ(ppm): 1.69 (t, 3H, CH_3), 2.08 (s, 6H, C(CH_3)$_2$), 4.42 (s, 3H, NCH_3), 4.73 (q, 2H, N^+CH_2), 5.79 (s, 1H, –CH═), 7.53–7.55 (m, 1H, ArH), 7.60 (d, J = 8.0 Hz, 1H, ArH), 7.78–7.81 (m, 1H, ArH), 7.83 (d, J = 8.0 Hz, 1H, ArH), 7.93–7.96 (m, 2H, ArH), 7.99 (d, J = 8.0 Hz, 1H, ArH), 8.08 (d, J = 8.8 Hz, 1H, ArH), 8.10 (d, J = 8.0 Hz, 1H, ArH), 8.39 (d, J = 8.8 Hz, 1H, ArH). ^{13}C NMR ($CDCl_3$, 400 MHz) δ(ppm): 181.1, 149.7, 145.7, 144.7, 141.9, 137.2, 134.3, 129.9, 129.3, 128.6, 128.3, 127.9, 126.8, 126.3, 122.2, 121.1, 95.4, 51.7, 44.3, 41.3, 31.66, 30.50, 19.9. IR (KBr) υ: 3023 (w, $\upsilon_{=CH}$) 2967, 2909, (m, υ_{CH}) 1578, 1557, 1446, 1435 (s, $\upsilon_{C=C}$, $\upsilon_{C=N}$), 969 (m, $\delta_{=CH}$), 849, 807 (s, $\delta_{=CH}$) cm^{-1}. MS (70 eV) m/z (%): 300 (M–I–C_2H_5, 100), 172 (23), 157 (12), 143 (25), 142 (14), 130 (10), 115 (9), 89 (4), 51 (2), 29 (7). Anal. Calcd. for $C_{23}H_{25}N_2I$ = 456.36: C, 60.53; H, 5.52; N, 6.14; Found: C, 60.49; H, 5.42; N, 6.09. UV–Vis (MeOH) λ_{max}: 473 nm. ε: 4.65×10^4 L mol^{-1} cm^{-1}.

2.4.3. 1,3′,3′-Trimethyl-1′- propyl-indo-2-quinocyanine iodide (**5c**)

Salmon pink powder, m.p.:228–229 °C. ^{1}H NMR (DMSO-d_6, 400 MHz) δ(ppm): 1.17 (t, 3H, CH_3), 2.06–2.11 (m, 8H, CH_2, C(CH_3)$_2$), 4.43 (s, 3H, NCH_3), 4.70 (t, 2H, N^+CH_2), 5.78 (s, 1H, –CH═), 7.51–7.53 (m, 1H, ArH), 7.61 (d, J = 8.0 Hz, 1H, ArH), 7.75–7.77 (m, 1H, ArH), 7.84 (d, J = 8.0 Hz, 1H, ArH), 7.93–7.97 (m, 2H, ArH), 7.99 (d, J = 8.0 Hz, 1H, ArH), 8.08 (d, J = 8.8 Hz, 1H, ArH), 8.11 (d, J = 8.0 Hz, 1H, ArH), 8.41 (d, J = 8.8 Hz, 1H, ArH). ^{13}C NMR ($CDCl_3$, 400 MHz) δ(ppm): 183.0, 152.6, 145.9, 143.1, 142.4, 136.7, 134.4, 129.5, 129.1, 129.0, 128.7, 128.5, 124.7, 127.5, 118.4, 116.5, 98.2, 60.9, 55.4, 47.2, 44.7, 33.5, 31.2, 15.6. IR (KBr) υ: 3027 (w, $\upsilon_{=CH}$) 2969, 2914 (m, υ_{CH}), 1587, 1554, 1458, 1431 (s, $\upsilon_{C=C}$, $\upsilon_{C=N}$), 968 (m, $\delta_{=CH}$), 847, 807 (s, $\delta_{=CH}$) cm^{-1}. MS (70 eV) m/z (%): 300 (M–I–C_3H_7, 100), 172 (23), 157 (16), 144 (27), 142 (17), 127 (6), 115 (12), 77 (6), 51 (7), 43 (3). Anal. Calcd. for $C_{24}H_{27}N_2I$ = 470.39: C, 61.28; H, 5.79; N, 5.96; Found: C, 61.15; H, 5.75; N, 5.89. UV–Vis (MeOH) λ_{max}: 478 nm. ε: 4.71×10^4 L mol^{-1} cm^{-1}.

2.4.4. 1′-Butyl-1,3′,3′-trimethyl-indo-2-quinocyanine iodide (**5d**)

Salmon pink solid, m.p.: 197–198 °C. ^{1}H NMR (DMSO-d_6, 400 MHz) δ(ppm): 1.02 (t, 3H, CH_3), 1.64–1.67 (m, 2H, CH_2), 2.05–2.10 (m, 8H, CH_2, C(CH_3)$_2$), 4.44 (s, 3H, NCH_3), 4.71 (t, 2H, N^+CH_2), 5.78 (s, 1H, –CH═), 7.51–7.53 (m, 1H, ArH), 7.61 (d, J = 8.0 Hz, 1H,

Table 1
The reaction conditions for the synthesis of dyes **5a–5d**.

Dyes	R	Power (W)	Time (min)	Yield (%)
5a	CH_3	252	15	58
5b	C_2H_5	252	15	48
5c	C_3H_7	252	18	56
5d	C_4H_9	252	18	59

Table 2
Effects of microwave power and irradiation time on yields of dye **5a**.

Power (W)	Time (min)	Yield (%)
126	15	0
175	9	33
252	6	34
252	9	53
252	15	58
252	18	59
252	24	59
406	3	30
406	9	17

ArH) 7.76–7.78 (m, 1H, ArH), 7.85 (d, $J = 8.0$ Hz, 1H, ArH), 7.93–7.97 (m, 2H, ArH), 7.99 (d, $J = 8.0$ Hz, 1H, ArH), 8.08 (d, $J = 8.8$ Hz, 1H, ArH), 8.11 (d, $J = 8.0$ Hz, 1H, ArH), 8.41 (d, $J = 8.8$ Hz, 1H, ArH). ^{13}C NMR ($CDCl_3$, 400 MHz) δ(ppm): 182.7, 147.6, 145.2, 145.0, 140.6, 137.8, 134.4, 129.5, 129.3, 129.1, 128.8, 128.0, 127.5, 123.8, 117.2, 113.1, 94.6, 56.2, 43.0, 39.6, 36.3, 30.8, 29.2, 19.3, 14.3. IR (KBr) υ: 3026 (w, $\upsilon_{=CH}$) 2966, 2908, (m, υ_{CH}) 1596, 1557, 1469, 1430 (s, $\upsilon_{C=C}$, $\upsilon_{C=N}$), 973 (m, $\delta_{=CH}$), 851, 803 (s, $\delta_{=CH}$) cm^{-1}. MS (70 eV) m/z (%): 300 (M–I–C_4H_9, 100), 172 (20), 157 (28), 143 (26), 142 (18), 127 (8), 115 (8), 77 (2), 57 (8), 43 (3). Anal. Calcd. for $C_{25}H_{29}N_2I = 484.42$: C, 61.99; H, 6.03; N, 5.78; Found: C, 62.04; H, 5.95; N, 5.65. UV–Vis (MeOH) λ_{max}: 479 nm. ε: 4.79×10^4 L mol^{-1} cm^{-1}.

2.5. Determination of the UV–Vis absorption properties

The UV–Vis spectra of dye **5a** in several common solvents were determinated. All the data were examined at room temperature and recorded using 1 cm quartz cells on a Shimadzu UV-1700 UV–Vis spectrometer. A stock solution (10^{-3} mol/L) of the dye was diluted to a suitable volume in order to obtain the required concentration. All of the physical constants of solvents and the absorption spectral data of dye **5a** are listed in Table 3.

3. Results and discussion

3.1. Synthesis

The synthetic conditions of dyes **5a–5d** are listed in Table 1. It could be seen that the condensation time of indole quaternary salts and 2-methylthio quinoline quaternary salt slightly increased with lengthening the carbon chain of the substituents within a certain microwave irradiation power. This indicated that the substituents of quaternary salts had little effect on the synthesis of the dyes. Compared with the Solvent Refluxing Method, the microwave radiation technique had a better yield and a shorter reaction time. Such as the synthesis of dye **5a**, the yield could reach to 59% with a power of 252 W microwave radiation for 15 min. However, it took nearly 2 h and the yield was only 21% using the conventional method [19].

Table 2 lists the effect of microwave power and irradiation time on yield of dye **5a**. It could be found that the yield increased

Table 3
The physical constants and the spectral data of dye **5a** in different solvents.

No.	Solvent	Refractive index/n	λ_{max} (nm)	Dielectric constant/ε	$\varepsilon \times 10^{-4}$ (L mol^{-1} cm^{-1})	$\lambda^{-1} \times 10^3$ (cm^{-1})
1	Acetone	1.359	440	20.7	3.9	2.27
2	Toluene	1.496	460	2.38	1.5	2.17
3	Methanol	1.329	471	32.63	4.7	2.12
4	Petroleum ether	1.442	441	1.8	2.6	2.27
5	Chloroform	1.446	461	4.9	5.0	2.17
6	Water	1.333	439	78.39	3.7	2.28

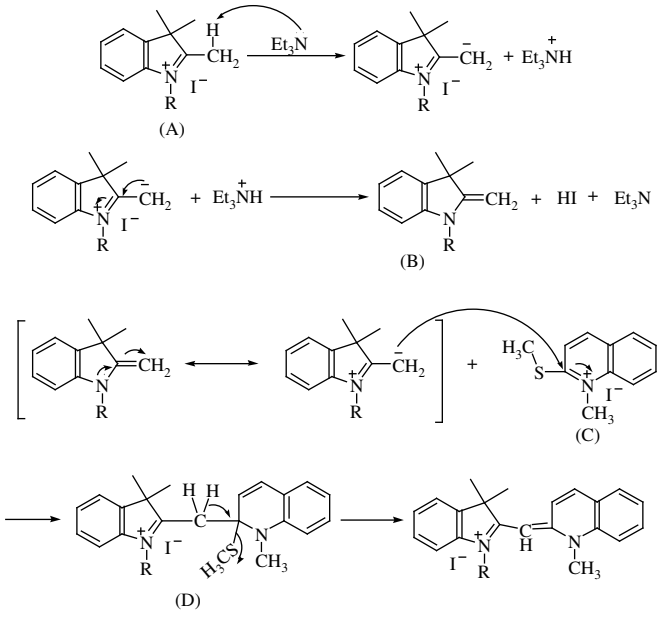

Fig. 2. The possible reaction mechanism of dyes **5a–5d.**

obviously with prolonging irradiation time within a certain power, but it no longer increased when irradiation time achieved 18 min. From Table 2, it could also be found that no reaction happened under lower power and the reaction time became shorter with the increase of the microwave power. This indicated that the greater the microwave radiation power, the faster the reaction rate. Carbonized phenomenon would occur and the yield would be decreased when the microwave power was excessively high.

It could be found that the kind of catalyst had great influence on the synthesis of four dyes in our experiment. Piperidine, pyridine, sodium acetate and triethylamine had been chosen as a catalyst, respectively. It was found that the reaction mixture rapidly became viscous and reaction couldn't continue when piperidine was added. This might be due to the strong basicity of piperidine. It was still not successful to use pyridine in the synthetic process, which was attributed to the weak basicity of pyridine. Though the dyes could be obtained when sodium acetate

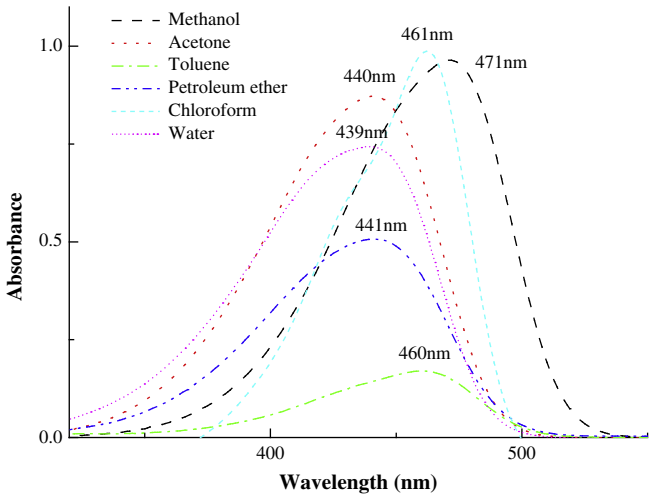

Fig. 3. UV–Vis absorption spectra of dye **5a** in different solvents.

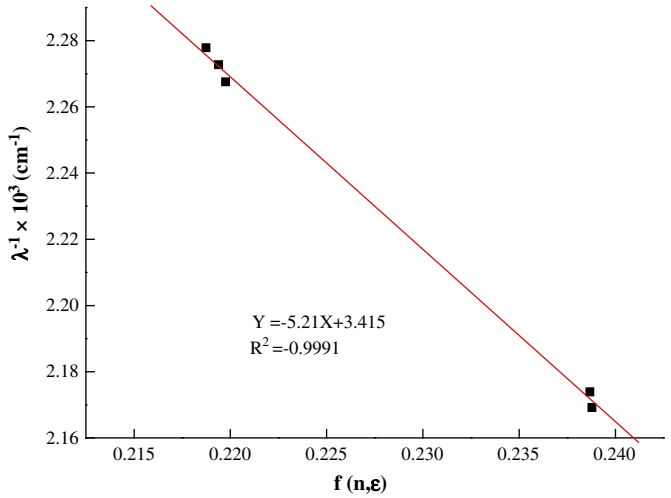

Fig. 4. Correlation of wavenumbers $1/\lambda$ in various solvents vs. $f(n,\varepsilon)$ of dye **5a**.

was used as a catalyst, the yield wasn't ideal. It was better to use triethylamine as a catalyst, but the control of catalyst amount in the condensation should be strict.

3.2. The possible reaction mechanism of dyes ***5a–5d***

The possible formation mechanism of dyes (**5a–5d**) is proposed as Fig. 2. In the first step, the hydrogen at 2-methyl of 2,3,3-trimethylindole quaternary salts has activity and is abstracted by catalyst Et_3N, yielding indoline. The latter step undergoes nucleophilic addition reaction of the 2-methylthio quinoline quaternary salt, resulting in adducts (D), then followed by an elimination process to produce the desired dyes.

3.3. The UV–Vis spectra of dye ***5a*** in different solvent

The absorption spectral data recorded on dye **5a** in different solvents are listed in Table 3, and the UV–Vis absorption spectral graphic of dye **5a** in different solvents is shown in Fig. 3.

As could be seen from Fig. 3, the maximum absorption wavelength, molar extinction coefficient and peak profile of dye **5a** in different solvents were obviously different. The dye was in single molecular state in methanol, water, acetone, petroleum and toluene, respectively. The peak profile of the dye changed slightly in the chloroform solution, which was attributed to the formation of the aggregated state. The molar extinction coefficient significantly decreased in the non-polar solvent like toluene. In order to conduct a preliminary study of the relationship between absorption of dye **5a** and solvent physical constants, the drafting result of $1/\lambda$ with the Bayliss function [20] $f(n,\varepsilon) = (n^2-1)/(2n^2-1) + 0.5\times(\varepsilon-1)/(\varepsilon+1)$ is shown as Fig. 4, where the wave number $1/\lambda$ is calculated from the experimental λ_{max}. It could be found that the absorption wave number was in the trend of declining with the increment of $f(n,\varepsilon)$ of different solvents. The correlation relationship between $1/\lambda$ and $f(n,\varepsilon)$ was satisfactory. This indicated that absorption of dye **5a** was related to refractive index and dielectric constant of these solvents.

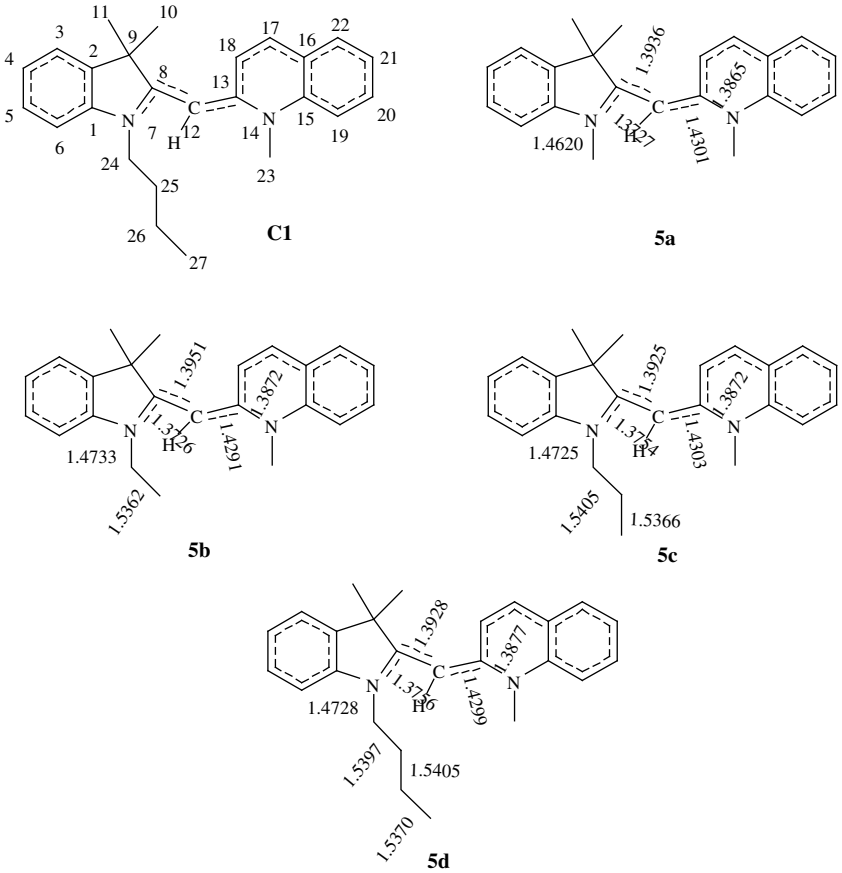

Fig. 5. The selected bond lengths (Å) of four dyes according to the B3LYP/6-31G level.

Table 4
The selected bond angles (°) and dihedral angles (°) of dyes **5a–5d** obtained according to the B3LYP/6-31G level.

	5a[a]	5b[a]	5c[a]	5d[a]
Bond angles				
1, 7, 24	123.0	122.1	122.3	122.3
8, 7, 24	124.8	125.8	125.7	125.8
8, 12, 13	130.5	130.4	130.8	131.0
13, 14, 15	122.5	122.5	122.5	122.6
13, 14, 23	119.3	119.3	119.3	119.4
12, 13, 18	123.3	123.4	123.4	123.6
Dihedral angles				
2, 1, 7, 24	−179.7	−180.0	−179.3	−179.5
24, 7, 8, 9	177.4	178.0	178.2	177.6
7, 8, 12, 13	168.2	166.7	169.7	170.9
8, 12, 13, 18	−37.9	−37.6	−40.3	−39.5
12, 13, 14, 15	169.4	169.1	168.8	169.2
12, 13, 14, 23	−13.1	−13.4	−13.7	−13.6
13, 14, 15, 16	6.9	7.0	6.6	6.8
13, 14, 15, 19	−173.2	−173.0	−173.4	−173.3

[a] The atom labels are marked in Fig. 5.

4. Theoretical studies

In this paper, the full geometry optimization, the lowest energy transitions, the absorption spectra and the resonance frequency calculation of four monomethine cyanine dyes with indole nucleus were calculated with adiabatic approximation of the TD-DFT using two hybrid exchange-correlation functionals, B3LYP [21] and PBE1PBE [22] including 20% and 25% of Hartree–Fock (HF) exchange, respectively. The geometries were fully optimized at the DFT level using 6-31G basis set. The solvent polarity effects were also taken into account at the B3LYP/6-31G and PBE1PBE/6-31G level. In this model, the dye molecule was embedded in a cavity surrounded by an infinite dielectric with the value of the desired solvent. The resonance frequency calculation of dye **5a** was also carried out at B3LYP/6-31G level. In our calculation, the anion was neglected as the experiment proved that the anion would not affect the spectra of the cationic dyes. Analytic frequency calculations were done to confirm the optimized structures to be an energy minimum. The results were compared with the experimental data and the error of calculation was estimated. All calculations reported in this work were realized with the Gaussian 03 program [23].

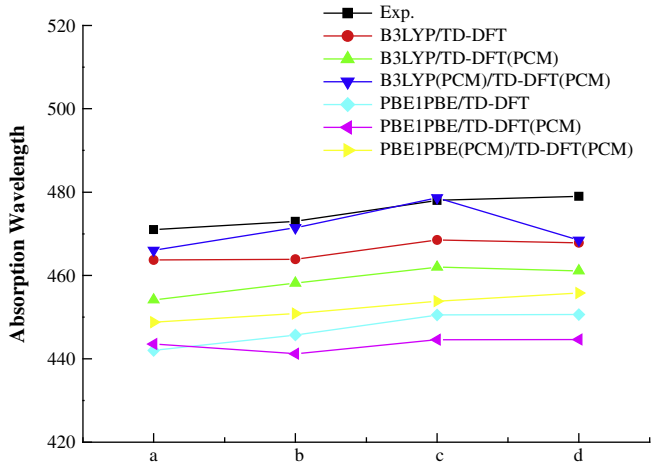

Fig. 6. Plot of experimental and theoretical λ_{max} of four dyes in methanol.

Table 5
The comparison of λ_{max} (nm) obtained by calculation and experiment.

solvents	Route 1	Route 2	Opt.	Exp.
Water	443.30	449.02	427.67	439
Methanol	443.54	448.76	444.39	471
Acetone	437.93	448.16	432.64	440
Chloroform	449.75	456.43	459.41	461
Toluene	454.44	461.99	464.88	460

Route 1: PBE1PBE/TD-DFT (PCM).
Route 2: PBE1PBE (PCM)/TD-DFT (PCM).
Opt.: Multiple linear regression model.

4.1. Geometric structures and symmetries

The atom labels and bond lengths obtained using B3LYP/6-31G level are showed in Fig. 5. It could be seen that the carbon–nitrogen bond lengths of four dyes molecular skeleton were intermediate between typical C–N single (1.47 Å) and C=N double (1.27 Å) bonds. The carbon–carbon bond lengths were intermediate between typical C–C single (1.54 Å) and C=C double (1.34 Å) bonds. The data showed that the π electrons in four dye molecules were basically delocalized. The selected bond angles and the dihedral angles of the four dyes are listed in Table 4. It could be seen that nearly all C–C–C bond angles were close to 120°. The torsion angles D(8, 12, 13, 18) of four dyes were −37.9° for **5a**, −37.6° for **5b**, −40.3° for **5c**, −39.5° for **5d** and D(7, 8, 12, 13) were 168.2° for **5a**, 166.7° for **5b**, 169.7° for **5c**, 170.9° for **5d**, respectively. The data indicated that four dye molecules had poor planarity, which led to the weak conjugated degree of π–π bonds. The reason was suggested by the stereo effect of the two methyls at 3-bit of indole ring.

4.2. UV–Vis absorption spectra

To obtain the reliable spectral data, several different DFT methods (B3LYP, PBE1PBE, B3LYP/PCM and PBE1PBE/PCM) at 6-31G basis set were used for investigating the absorption spectra of four dyes, and the linear regression analysis equation obtained in our previous research was used for studying theoretical results of the absorption maximum in different solvents.

4.2.1. Methodological study

Plot of experimental and theoretical λ_{max} of four dyes is shown in Fig. 6. It could be seen that the λ_{max} obtained by pure PBE1PBE or B3LYP method all significantly deviated the experimental data. The error between calculating and experiment result was in the range of −27.3 nm to −29.0 nm for PBE1PBE and −7.3 nm to −11.8 nm for B3LYP.

The comparison of absolute deviation for each dye molecule revealed that B3LYP method was more suitable than PBE1PBE method for studying the absorption spectra of four dyes. The introduction of a solvent reaction field and the individual combination of PCM and PBE1PBE, B3LYP method led to the much

Table 6
Main orbital compositions and excitation energies of dyes **5a–5d**.

Dyes	State	Transition feature	B3LYP/PCM[a]		
			Transition character[b]	ΔE (eV)	f
5a	^{1}A	π → π*	H → L (83.8%)	2.66 eV	f = 0.6660
5b	^{1}A	π → π*	H → L (83.7%)	2.63 eV	f = 0.6554
5c	^{1}A	π → π*	H → L (84.1%)	2.59 eV	f = 0.6214
5d	^{1}A	π → π*	H → L (83.5%)	2.65 eV	f = 0.6761

[a] Solvent is methanol.
[b] H and L stand for HOMO and LUMO respectively, and the proportion of the main transition is given in parenthesis.

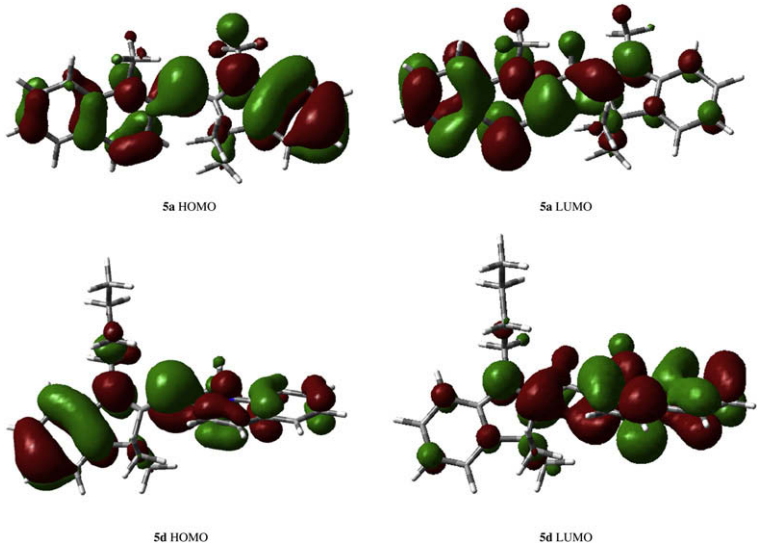

Fig. 7. Sketch of the main molecular orbitals for dye **5a** and **5d** obtained at the B3LYP(PCM)/6-31G level.

closer results with the experimental values. PBE1PBE/TD-DFT(PCM) and B3LYP/TD-DFT(PCM) were on the basis of gas-phase optimized geometries for spectra calculations in the solvent, while PBE1PBE(PCM)/TD-DFT(PCM) and B3LYP(PCM)/TD-DFT(PCM) used the solvated geometries for TD-DFT/PCM calculations. The λ_{max} optimized by B3LYP(PCM)/TD-DFT(PCM) reduced the absolute deviation to −5.0 nm for dye **5a**, −1.6 nm for dye **5b**, 0.6 nm for dye **5c**, and 10.5 nm for dye **5d**. It indicated that the accuracy was remarkably increased when the solvent effects was taken into account. In addition, in our calculation, the first excited singlet state was the only allowed state with the strongest oscillator strength and corresponded to $\pi \rightarrow \pi^*$ excitation of solely HOMO to LUMO.

4.2.2. Application of multiple linear regression model

Multiple linear regression attempts to model the relationship between two or more explanatory variables and a response variable by fitting a linear equation to observed data. In the previous study of our team, multiple linear regression model was applied to several series of dye molecules in order to explore the effects of solvent on absorption spectra and test the theoretical approach against the available experimental results.

A multiple linear regression model [24], which could significantly reduce the deviation between optimized and experimental λ_{max}, was formulated as:

$$Opt.\,(\lambda_{max}) = -112.24 + 3.00\,\lambda_{max}(Route\ 1) - 1.70\,\lambda_{max}(Route\ 2) - 0.34\varepsilon$$

where the explanatory variables stood for the λ_{max} calculated by Route 1 and Route 2, and ε was solvent dielectric constant. In this paper, Route 1 referred to the λ_{max} of dye **5a** obtained from PBE1PBE/TD-DFT (PCM) method and Route 2 referred to the λ_{max} of dye **5a** obtained from PBE1PBE (PCM)/TD-DFT (PCM) method, respectively. Five different solvents were considered including water, methanol, acetone, chloroform, and toluene (their dielectric constant amounts to 78.39, 32.63, 20.70, 4.90 and 2.38, respectively). The absorption maximum (λ_{max}) of dye **5a** obtained by the TD-PBE1PBE/PCM/6-31G and the λ_{max} obtained by the multiple regression model are presented in Table 5. It could be seen that with the exception of methanol, the maximal deviation between optimized and experimental λ_{max} decreased to about −1.6 to −11.3 nm for the other solvents. Although relative deviation of λ_{max} in methanol was −5.6%, it was still reliable to such a large conjugated system of dye molecule. This definitively confirmed the

Table 7
The comparison of calculated and experimental infrared data of dye **5a**.

No.	Calcd.			Exp.		Vibratory feature
	Non-scaled	Scaled	Int. (IR)	Freq.	Int. (IR)[a]	
1	3130	3009	11.4	3010	w	$\upsilon_{=CH}$
2	3060	2942	26.0	2973	m	υ_{C-H}
3	3050	2932	22.5	2901	m	υ_{C-H}
4	1610	1548	443.9	1593	v	$\upsilon_{C=C}$
5	1600	1538	608.1	1566	v	$\upsilon_{C=C}$
6	1550	1490	186.8	1467	s	$\upsilon_{C=C}$, $\upsilon_{C=N}$
7	1540	1480	108.6	1428	s	$\upsilon_{C=C}$, $\upsilon_{C=N}$
8	980	942	19.0	968	m	$\delta_{=CH}$
9	880	846	75.6	846	s	$\delta_{=CH}$

Frequencies in cm^{-1}, scaling factor using 0.9613 [25][a]m: middle, s: strong, v: very strong, w: weak.

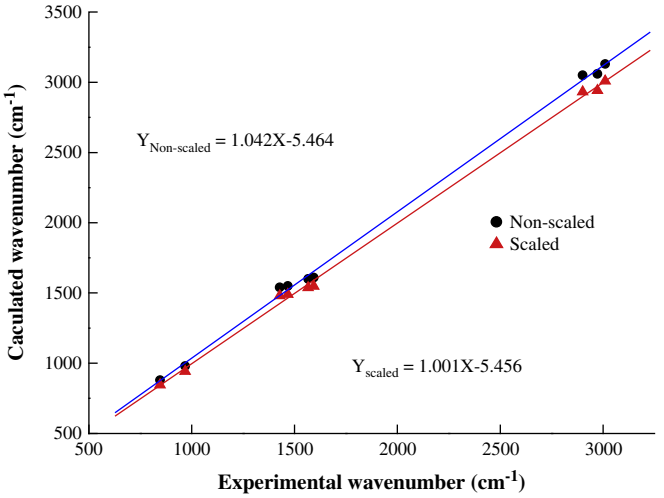

Fig. 8. Consistency of the wavenumbers of calculated and experimental IR spectra main peaks of dye **5a**.

validity of the equation for a quantitative evaluation of the λ_{max} of monomethine cyanine dyes with indole nucleus. The multiple linear regression model could be used as a tool for scientific workers in the future research.

4.2.3. Assignment of the calculated transition

Table 6 lists the main orbital compositions of the computed lower-lying singlet excited states and transition feature of four dye molecules obtained at the B3LYP(PCM)/6-31G level. It was found that the lowest energy absorption in the dyes could be attributed to the electronic $\pi \rightarrow \pi^*$ transition from HOMO to LUMO. It could also be found that the frontier orbitals of dye **5a**–**5d** were nearly the same in our calculation. Took dye **5a** and **5d** for example, the HOMO of dye **5a** and **5d** were mainly localized on the whole molecular skeleton, the LUMO of dye **5a** and **5d** were mainly distributed at quinoline nucleus (Fig. 7). The HOMO → LUMO transition of the two dyes was from the indole group to the quinoline moiety.

4.3. Calculation and experimental comparison of IR spectra

The full geometry optimization and the resonance frequency calculation of dye **5a** were carried out at B3LYP/6-31G level. The comparison of calculated and experimental data of IR spectra is listed in Table 7.

From Table 7, we could see that the calculated IR spectral data were slightly higher than the experimental value. The reason suggested here was that the result obtained by the calculation was harmonic oscillation frequency, while the experimental value contained the anharmonic oscillation frequency. The data were modified using 0.9613 [25] as the frequency scaling factor, and the consistent relation graph between calculated and experimental data of dye **5a** is shown as Fig. 8. It could be seen that the linear slope and intercept were 1.042, −5.464 for the non-scaled data and 1.001, −5.456 for the scaled, respectively. This explained that the error was decreased for the introduction of the frequency scaling factor, and the calculated data was in good agreement with the experimental value.

5. Conclusions

A rapid and highly efficient method for the synthesis of monomethine cyanine dyes with indole nucleus is described under solvent-free microwave irradiation by the condensation of indole quaternary salts and 2-methylthio quinoline quaternary salt in the presence of triethylamine. The absorption of prepared dyes is in the region of 471–479 nm. In addition, B3LYP/PCM method gives a reliable description of the molecular absorption characters and reproduces the $\pi \rightarrow \pi^*$ type absorption bands of the dyes. Multiple linear regression model obtained in the previous work is also applied to examine the interrelationships between calculated and experimental λ_{max} in five solvents. The estimated relative deviation in the λ_{max} is about −0.35% to −5.6%. Resonance frequency calculation is carried out to study the IR spectra of self-synthesized dyes, and the calculated results are in good accordance with the experimental values.

Acknowledgement

We appreciate the financial support for this research by a grant from the Natural Science Foundation of Shaanxi Province (No. SJ08B04), the Special Science Research Foundation of the Education Committee of Shaanxi Province (No. 08JK458), NWU Doctorate Dissertation of Excellence Funds (08YYB04) and the Science Research Startup Foundation of Northwest University.

References

[1] Zhao WF, Saijo H, Kobayashi Y, Shiojiri M, Yan WP, Li Q, et al. Effects of thiacarbocyanine and indocarbo cyanine dye with different substituents on absorption to AgBr microcrystal and size distribution of J-aggregates. Photographic Science and Photochemistry 1997;15(4):327–34 [in Chinese].
[2] Liao WY, Lee MC, Huang CL, Yan CF, Cheng TR, Hu T, et al. Preparation of cyanine dye for high density optical recording disk. JP 2004219915, 2004.
[3] Umezawa K, Morita S, Takazawa K, Ando H, Ootera Y, Nakamura N, et al. Optical disk, information recording method, and information reproducing method. EP 1863026, 2007.
[4] Morishita D, Okitsu I, Uchida M, Kodaira T, Hiratsuka H, Horiuchi H, et al. Monomethine dye compound, optical information recording medium utilizing the compound and process for producing the same. EP 1734080, 2006.
[5] Deligeorgiev TG, Gadjev NI, Vasilev AA, Maximova VA, Timcheva II , Katerinopoulos HE, et al. Synthesis and properties of novel asymmetric monomethine cyanine dyes as non-covalent labels for nucleic acids. Dyes and Pigments 2007;75(2):466–73.
[6] Volkova KD, Kovalska VB, Balanda AO, Yu Losytskyy M, Golub AG, Vermeij RJ, et al. Specific fluorescent detection of fibrillar a-synuclein using mono- and trimethine cyanine dyes. Bioorganic & Medicinal Chemistry 2008;16:1452–9.
[7] Zhang XH, Wang LY, Nan ZX, Tan SH, Zhang ZX. Microwave-assisted solvent-free synthesis and spectral properties of some dimethine cyanine dyes as fluorescent dyes for DNA detection. Dyes and Pigments 2008;79(2):205–9.
[8] Zhao HL, Yuan HH, Lan MB. Application of cyanine dyes and related compounds as fluorescent probes and photodynamic therapy. Photographic Science and Photochemistry 2003;21(03):212–22.
[9] Delaey E, Van LF, De VD, Kamuhabwa A, Jacobs P, De WP. A comparative study of the photosensitizing characteristics of some cyanine dyes. Journal of Photochemistry and Photobiology, B: Biology 2000;55(1):27–36.
[10] Abd El-Aal RM, Younis M. Synthesis and antimicrobial activity of certain novel monomethine cyanine dyes. Dyes and Pigments 2004;60(3):205–14.
[11] Wang LY, Chen QW, Zhai GH, Wen ZY, Zhang ZX. Investigation of the structures and absorption spectra for some hemicyanine dyes with pyridine nucleus by TD-DFT/PCM approach. Journal of Molecular Structure: THEOCHEM 2006;778(1–3):15–20.
[12] Runge E, Gross EKU. Density-functional theory for time-dependent systems. Physical Review Letters 1984;52(12):997–1000.
[13] Gross EKU, Kohn W. Local density-functional theory of frequency-dependent linear response. Physical Review Letters 1985;55(26):2850–2.
[14] Oh D, Choe JI. DFT Study of p-tert-butylcalix [5] crown-6-ether complexed with alkylammonium ions. Bulletin of the Korean Chemical Society 2007;28(4):596–600.
[15] Kim K, Choe JI. DFT study of bis(crown-ether) analogue of Troger's base complexed with bisammonium ions: hydrogen bonds. Bulletin of the Korean Chemical Society 2006;27(11):1737–40.
[16] Wang LY, Chen QW, Zhai GH, Wen ZY, Zhang ZX. Theoretical study on the structures and absorption properties of styryl dyes with quinoline nucleus. Dyes and Pigments 2007;72(3):357–62.
[17] Wang W, Yao ZG. Synthesis and properties of squarylium cyanine dyes containing *N*-alkyl indole. Photographic Science and Photochemistry 1997;15(4):321–6 [in Chinese].
[18] Heilbron Ivan. Dictionary of organic compounds IV. Beijing: Science Press; 1966 [in Chinese].
[19] Ficken GE, Kendall JD. The reactivity of the alkylthio-group in nitrogen ring compounds. Part II: cyanine bases from 3,3-dimethyl-2-methylthio-3H-indole. Journal of the Chemical Society 1960:1529–36.
[20] West W, Geddes AL. The effects of solvents and of solid substrates on the visible molecular absorption spectrum of cyanine dyes. Journal of Physical Chemistry 1964;68(4):837–47.
[21] Becke AD. Density-functional thermochemistry. III: the role of exact exchange. The Journal of Chemical Physics 1993;98:5648–52.
[22] Perdew JP, Burke K, Ernzerhof M. Generalized gradient approximation made simple. Physical Review Letters 1996;77(18):3865–8.
[23] Frisch M, Trucks GW, Schlegel HB, Scuseria GE, Robb MA, Cheeseman JR, Montgomery JA, Vreven JT, Kudin KN, Burant JC, Millam JM, Iyengar SS, Tomasi J, Barone V, Mennucci B, Cossi M, Scalmani G, Rega N, Petersson GA, Nakatsuji H, Hada M, Ehara M, Toyota K, Fukuda R, Hasegawa J, Ishida M, Nakajima T, Honda Y, Kitao O, Nakai H, Klene M, Li X, Knox JE, Hratchian HP, Cross JB, Adamo C, Jaramillo J, Gomperts R, Stratmann RE, Yazyev O, Austin AJ, Cammi R, Pomelli C, Ochterski JW, Ayala PY, Morokuma K, Voth GA, Salvador P, Dannenberg JJ, Zakrzewski VG, Dapprich S, Daniels AD, Strain MC, Farkas O, Malick DK, Rabuck AD, Raghavachari K, Foresman JB, Ortiz JV, Cui Q, Baboul AG, Clifford S, Cioslowski J, Stefanov BB, Liu G, Liashenko A, Piskorz P, Komaromi I, Martin RL, Fox DJ, Keith T, Al-Laham MA, Peng CY, Nanayakkara A, Challacombe M, Gill PM, Wohnson B, Chen W, Wong MW, Gonzalez C, Pople JA. Gaussian 03. Revision B. 03. Pittsburgh, PA: Gaussian, Inc.; 2003.
[24] Zhang XH, Wang LY, Zhai GH, Wen ZY, Zhang ZX. Microwave-assisted solvent-free synthesis of some dimethine cyanine dyes, spectral properties and TD-DFT/PCM calculations. Bulletin of the Korean Chemical Society 2008;28(12):2382–8.
[25] Chen QW, Wang LY, Zhai GH, Wen ZY, Zhang ZX. Study on electronic spectra of 2-styryl-β-naphthathiazole dyes with time-dependent density functional theory. Acta Chimica Sinica 2005;63(1):39–43 [in Chinese].